Heliyon 7 (2021) e06701

Contents lists available at ScienceDirect

Heliyon

journal homepage: www.cell.com/heliyon

Research article

A longitudinal comparison in cynomolgus macaques of the effect of brimonidine on optic nerve neuropathy using diffusion tensor imaging magnetic resonance imaging and spectral domain optical coherence tomography

Nobuyuki Takahashi [a], Naoko Matsunaga [a], Takahiro Natsume [a], Chinatsu Kitazawa [a], Yoshitaka Itani [a], Aldric Hama [a,*], Ikuo Hayashi [b], Masamitsu Shimazawa [c], Hideaki Hara [c], Hiroyuki Takamatsu [a]

[a] Pharmacology, Hamamatsu Pharma Research, Inc., 1-3-7, Shinmiyakoda, Kita-ku, Hamamatsu, Shizuoka, 431-2103, Japan
[b] Hamamatsu Pharma Research USA, Inc., 4660 La Jolla Village Drive, San Diego, CA, 92122 USA
[c] Molecular Pharmacology, Department of Biofunctional Evaluation, Gifu Pharmaceutical University, 1-25-4 Daigaku-nishi, Gifu 501-1196, Japan

ARTICLE INFO

Keywords:
Laser-induced ocular hypertension
Optic nerve fractional anisotropy
Retinal nerve fiber layer thickness
Diffusion tensor imaging-magnetic resonance imaging
Spectral domain optic coherence tomography
Neuroprotection

ABSTRACT

Early detection of optic neuropathy is crucial for initiating treatment that could delay or prevent visual field loss. Preclinical studies have advanced a number of potential neuroprotective strategies to prevent retinal ganglion cell (RGC) degeneration, but none have successfully completed clinical trials. One issue related to the lack of preclinical to clinical translation is the lack of preclinical morphometric assessments that could be used to track neuroprotection, as well as neurodegeneration, over time within the same animal. Thus, to assess whether clinically used morphometric assessments can identify neuroprotection of RGC, the current study compared optic nerve fractional anisotropy (FA) obtained with diffusion tensor imaging (DTI) and retinal nerve fiber layer (RNFL) thickness measured with spectral domain optical coherence tomography (SD-OCT) to observe not only the early progression of RGC axonal degeneration but to also discern which imaging modality identifies signs of neuroprotection during treatment with the alpha-adrenoceptor agonist brimonidine. Elevated and sustained intraocular pressure (IOP) was observed following laser photocoagulation of the trabecular meshwork in one eye of nonhuman primates (NHP). Either brimonidine (0.1%) or control treatment was instilled twice daily for two months. In control-treated eyes, increased IOP, increased vertical cup-to-disc (C/D), reduced rim-to-disc (R/D) ratio, decreased RNFL thickness and decreased FA were observed. While IOP remained elevated during the course of the study, brimonidine tended to delay the progression of RNFL thinning. However, in the same animal, optic nerve FA did not appear to decline. Brimonidine treatment did not affect other measures of RGC axonal degeneration. The current findings demonstrate that early progression of optic neuropathy can be tracked over time in a nonhuman primate model of ocular hypertension using either DTI or SD-OCT. Furthermore, the delayed changes to RNFL thickness and FA appear to be a neuroprotective effect of brimonidine independent of its effect on IOP.

1. Introduction

Glaucoma is one of the leading causes of irreversible blindness worldwide which involves progressive degeneration of retinal ganglion cells (RGC) [1]. The axons of the RGC exit the eye via the optic disc and changes in axon number can be visualized via funduscopy as increased cup-to-disc ratio and decreased neuroretinal rim-to-disc ratio [2]. Furthermore, cells that are either presynaptic or postsynaptic to RGC undergo transynaptic degeneration—neural degeneration has been observed as distal as the primary visual cortex [3,4,5,6]. Thus, glaucoma can be considered a multifocal degenerative neuropathy.

As a multifocal degenerative neuropathy, early detection of optic nerve neuropathy and treatment to slow or halt the neurodegenerative process may prevent visual field loss [7]. With respect to potential treatments, preclinical studies have suggested a number of mechanisms mediating RGC degeneration, including glutamate-induced

* Corresponding author.
E-mail address: aldric-hama@hpharma.jp (A. Hama).

https://doi.org/10.1016/j.heliyon.2021.e06701
Received 10 February 2020; Received in revised form 4 January 2021; Accepted 31 March 2021

neurotoxicity, reduced axonal transport of trophic factors, ischemia-related injury and mitochondrial dysfunction through oxidative stress [4,8]. Targeting these mechanisms, alone or in combination, could enhance survival and functioning of RGC.

With respect to timing of interventions, however, the crucial period between responsiveness and non-responsiveness of RGC to treatment has yet to be defined. While assessing optic nerve head topography is the standard method in observing glaucomatous neuropathy progression, this approach is not sensitive to gradual RGC loss and image rating agreement between raters is low [9,10]. In most preclinical studies, loss of retinal ganglion cell bodies and axons are quantified from histological preparations to assess disease progression and neuroprotective effects of potential treatments. However, this precludes longitudinal studies within the same animal.

Structural assessment of RGC axons, contained within the retinal nerve fiber layer (RNFL), with spectral domain optical coherence tomography (SD-OCT) has been suggested as an objective and quantitative method of detecting and tracking glaucomatous disease progression [11]. Furthermore, the rate of RNFL thinning over time measured by SD-OCT appears to predict future visual loss [12]. Nonetheless, subtle neuroanatomical changes in early glaucoma may be below the level of detection with SD-OCT [11,13].

Changes in water molecule diffusion within optic nerve during glaucomatous neuropathy suggests disruption in tissue microstructure. Diffusion tensor imaging (DTI) measures water diffusion through tissue and fractional anisotropy (FA) reflects anisotropic movement of water molecules within tissues. In glaucoma patients, decreased FA suggests decreased water diffusion due to decreased optic nerve structural integrity [14]. An apparent association between FA and glaucomatous severity, as functionally assessed by visual field loss, has been reported. Furthermore, it appears that optic nerve FA can be used to distinguish between mild and severe glaucomatous damage [15]. In macaques with experimentally induced glaucoma, optic nerve neurofilament density positively correlates with FA—decreased FA suggests decreased RGC axons [15,16]. Therefore, optic nerve FA could be used as a biomarker for glaucomatous neuropathy [17,18]. While DTI could have utility as a longitudinal method of following RGC loss, few studies have examined its potential in tracking treatment effects over time.

Brimonidine, a highly selective α_2-adrenoceptor agonist, is used to reduce IOP by inhibiting adenylate cyclase, thereby reducing aqueous humor synthesis, while at the same time moderately enhancing outflow through the trabecular and the uveoscleral pathways. Brimonidine appears to have a neuroprotective mechanism of action as well [19,20,21,22]. The neuroprotective effect of brimonidine has yet to be fully understood but it appears to modulate glutamate transporters and ionotropic N-methyl--D-aspartate (NMDA) receptors, thereby preventing RGC apoptosis and axonal loss by blocking cellular excitotoxity by excitatory amino acids [23]. Whether such a similar mechanism exists in the human eye and can be pharmacologically modulated to prevent RGC degeneration has yet to be determined. In rodent models of experimentally elevated IOP, systemic brimonidine prevented the loss of RGC without affecting IOP—whether there is a neuroprotective effect of brimonidine in species that are phylogenetically closer to humans than rodents has yet to be demonstrated [24].

The current study compared DTI and SD-OCT in their ability to detect early signs of neurodegeneration, in the optic nerve and RNFL, respectively, in a macaque model of ocular hypertension. In addition, these imaging modalities were compared and contrasted in their ability to distinguish a potential neuroprotective effect of brimonidine over time.

2. Materials and methods

2.1. Animals

Cynomolgus macaques (*Macaca fascicularis*) were obtained from Shin Nippon Biomedical Laboratories, Ltd (Kagoshima, Japan) and Eve Bioscience., Ltd (Wakayama, Japan). All study procedures were reviewed and approved by the Hamamatsu Pharma Research, Inc. Animal Care and Use Committee. All procedures were carried out in accordance according to the guidelines within the *Guide for the Care and Use of Laboratory Animals* [25] and consistent with the Association for Research in Vision and Ophthalmology Statement for the Use of Animal in Ophthalmic and Vision Research.

Animals were housed individually for the duration of the study and were provided with environmental enrichment, including manipulanda. To facilitate acclimation to humans, staff hand-fed treats to the macaques at least once per week. Macaques were fed about 100 g/animal per day of standard nonhuman primate chow (Oriental Yeast Co., Ltd., Tokyo, Japan), which was supplemented weekly with either fresh fruits or vegetables. Macaques had free access to tap water via an automatic watering system.

Environmental conditions of the holding rooms were under automatic control and followed standards described in the *Guide for the Care and Use of Laboratory Animals* [25]. A 12-hour light-dark cycle, with lights on at 7:00 AM, was used in the animal housing room. Studies were carried out during the light hours, between 8:00 AM and 4:00 PM. The facility is fully accredited by AAALAC International.

2.2. Ocular hypertension model

Laser photocoagulation was used to induce a unilateral ocular hypertension. Overt time, robust glaucomatous neuropathy is evident, including changes in C/D and R/D ratios. Pathology is highlighted by a consistent loss of RGC and axonal degeneration over time [17,26]. It should be noted that the current model is an acutely induced-model, whereas clinical glaucomatous neuropathy may develop over an extended period of time.

Ocular hypertension of the left eye was induced by laser photocoagulation of the trabecular meshwork [26,27] with a 532 nm green laser photocoagulator (GYC-500, Nidek Co. Ltd., Gamagori, Japan) attached to a slit-lamp microscope (SL-1800, Nidek Co. Ltd.). The right eye did not undergo laser photocoagulation and served as a normotensive control.

Macaques were anesthetized with a mixture of ketamine (15 mg/kg, i.m.; Daiich-Sankyo, Tokyo, Japan) and xylazine (2 mg/kg, i.m.; Bayer Yakuhin, Osaka, Japan). Local anesthetic oxybuprocaine HCl (Benoxil® ophthalmic solution 0.4%; Santen Pharmaceuticals, Osaka, Japan) was applied to the cornea. A single-mirror Gonio lens (OSMGA, Ocular Instruments, WA, USA) filled with a hydroxyethylcellulose solution (Scopisol®; Senju Pharmaceutical, Osaka, Japan) was placed on the eye to undergo laser photocoagulation. The laser was focused on the mid-portion of the trabecular meshwork and a total of 50–150 laser-beam spots (spot size 100 μm, 1000 mW, exposure time 0.2 s) were applied to 360^o of the trabecular meshwork.

Using the same procedure, a second laser treatment of the same eye was performed two weeks later.

Measurement of ocular parameters started beginning one week after the second laser treatment (see 2.4. Measurement of ocular parameters.)

2.3. Brimonidine treatment

Treatment with either brimonidine or artificial tears began one week (Week 1) after the second laser photocoagulation, following measurement of ocular parameters (see below). Either brimonidine (0.1%, Senju Pharmaceutical, Osaka, Japan) or control treatment (artificial tears (Soft Santear®, Santen Pharmaceutical)) was topically instilled twice per day for the duration of the study period. Six macaques received brimonidine in both eyes (i.e., the ipsilateral, hypertensive eye and the contralateral, normotensive eye) and six macaques received control treatment in both eyes. Measurement of IOP following long-term brimonidine treatment was performed prior to the morning instillation.

To observe the short-term effect of brimonidine treatment on IOP, IOP was measured 1, 2, 4, 6, and 8 h following instillation. Following IOP measurement at 8 h after instillation, a second instillation of brimonidine was done and IOP was measured 1 and 2 h after instillation (or 9 and 10 h after the first instillation.)

2.4. Measurement of ocular parameters

Intraocular pressure, vertical cup-to-disc (C/D) ratio and minimum rim-to-disc (R/D) ratio, retinal nerve fiber layer (RNFL) thickness and fractional anisotropy (FA) were measured 1, 2, 3, 4, 6 and 8 weeks after the second laser trabeculoplasty.

2.4.1. Intraocular pressure measurement (IOP)

Intraocular pressure was measured with a hand held tonometer TonoVet ® (Icare Finland Oy, Vantaa, Finland) while the macaques were awake and restrained in a monkey chair. The average of three measurements (mmHg) was reported as the final IOP. The change in IOP was calculated by subtracting the post-dose IOP from the pre-dose IOP.

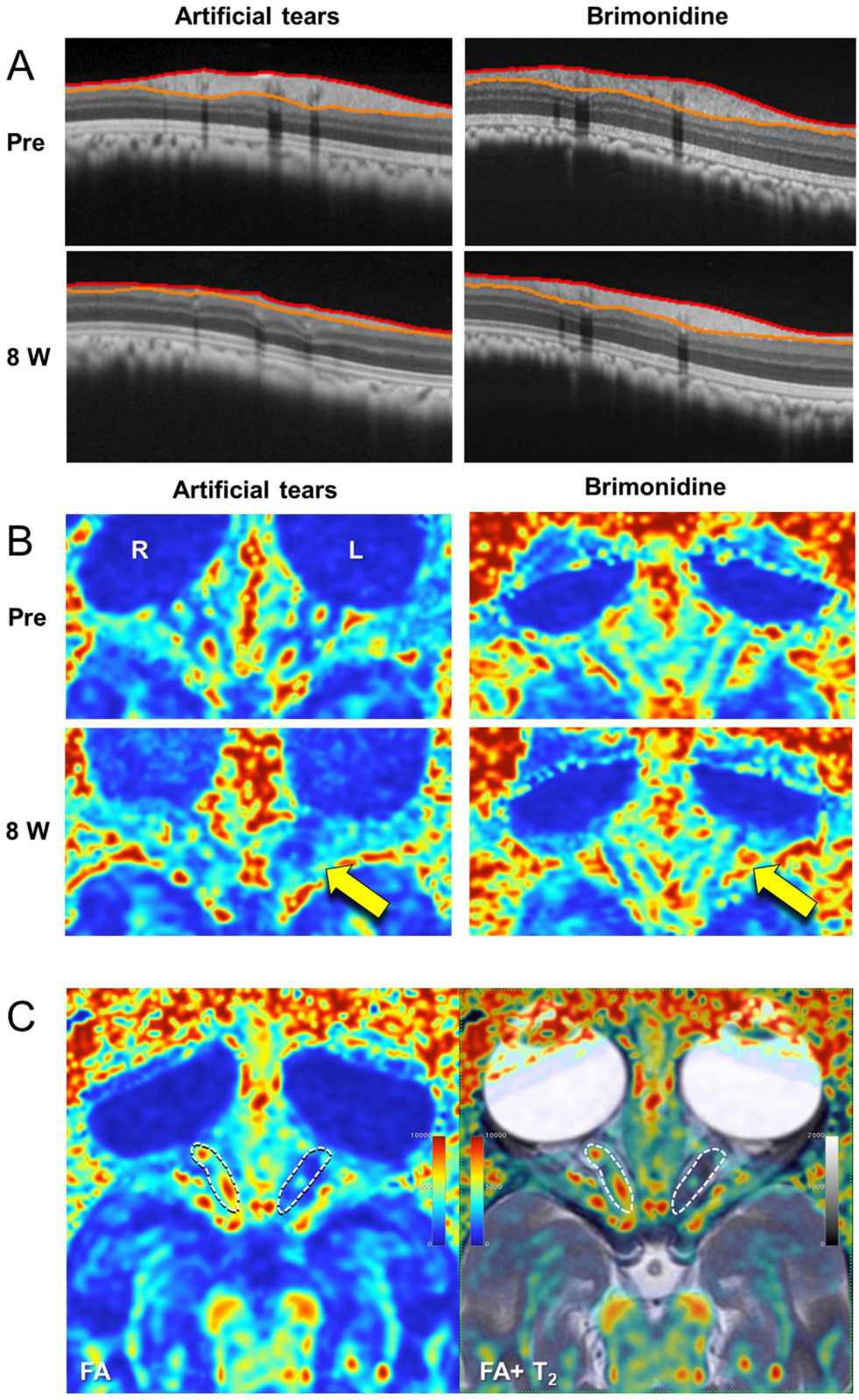

Figure 1. Representative spectral domain optical coherence tomography (SD-OCT) B-scan images and DTI images of glaucomatous eyes before (Pre) and eight weeks after (8W) treatment with artificial tears (left) or brimonidine (right). (A) Spectral domain optical coherence tomography B-scan images before and eight weeks after treatment with either artificial tears or brimonidine. The boundaries of the RNFL are outlined in red and orange. (B) DTI axial section of from a macaque with a normotensive right (R) and glaucomatous left (L) eye. Yellow arrows indicate location of glaucomatous optic nerve. (C) Representative DTI image (left) combined with a T2 weighted (right) image delineating anatomical structures. Region of interests (dotted lines) were overlaid on each subject's FA map and a mean FA value for each region was calculated.

2.4.2. Spectral domain optical coherence tomography (SD-OCT)

Spectral domain optical coherence tomography (RS-3000 advance; Nidek) scans of the optic nerve head were performed in both eyes of animals to quantitatively measure RNFL thickness (μm), vertical C/D ratio and minimum R/D ratio. Before imaging, animals were anesthetized with ketamine (15 mg/kg, i.m.) and xylazine (2 mg/kg, i.m.). Anesthesia was reversed with atipamezole (0.4 mg/kg, i.m.; Meiji Seika Pharma, Tokyo, Japan) at the end of the procedure. A disc map scan pattern, 512 points x 128 points, within a 6 × 6 mm square, was centered on the optic nerve head. Internal software segmented and calculated vertical C/D ratio and minimum R/D ratio. A disc circle scan pattern, 3.45 mm diameter centered on the optic nerve head, 1024 points, was used to create a papillary RNFL map. The RNFL thickness (μm) was the average of the sectors calculated with software installed in the OCT. Retinal nerve fiber layer thickness was determined automatically, but all the images were checked and manually corrected if there were any errors. Images greater than signal strength index (SSI) greater than 8 (maximum 10) were accepted for analysis.

Representative SD-OCT RNFL images before and 8 weeks after the second laser photocoagulation with artificial tears treatment and with brimonidine treatment are shown in Figure 1A.

2.4.3. Diffusion tensor magnetic resonance imaging

To obtain fractional anisotropy (FA) values, diffusion tensor images (DTI) were acquired using a 3.0T MRI system (GE Signa HDxt 3.0T MRI system (GE Healthcare, Milwaukee, WI, USA)) equipped with an 8-channel head coil. During DTI scanning, animals were anesthetized using pentobarbital (5 mg/kg, i.v.; Kyoritsu Seiyaku Co., Ltd., Tokyo, Japan), and the heads were supported by an acrylic head fixture (MATSUI Co., Ltd., Aichi, Japan). The anatomical MRI protocols consisted of a T2-weighted fast recovery fast spin echo (FRFSE) sequence (repetition time (TR)/echo time (TE), 3000.0/96.2 ms; number of averages, 1; flip angle, 90°; echo train length (ETL), 21; field of view (FOV), 100 mm × 100 mm; matrix, 320 × 256; slice thickness/interval, 2.0/0.0 mm). The DTI data were acquired using a multi-shot spin-echo type EPI sequence (number of shot, 2; TR/TE, 17000.0/102.4 ms; number of averages, 2; FA, 90°; FOV, 100 mm × 100 mm; matrix, 128 × 128; slice thickness/interval, 2.4/0.0 mm, diffusion-weighted gradients of 28 directions, maximal diffusion-weighted factor, b = 1000 s/mm^2). Representative axial diffusion tensor images of optic nerve before and eight weeks after the second laser photocoagulation, with either artificial tears or brimonidine treatment, are shown in Figure 1B.

2.4.3.1. MRI image analysis. The DTI datasets were processed with FuncTool software on a GE Healthcare workstation. Fractional anisotropy was computed by fitting with a diffusion tensor model [28]. Datasets were automatically corrected for distortions and co-registered on T2-weighted images, and the FA values were calculated using FuncTool. The ROIs were manually drawn on the right (normotensive) and left (glaucomatous) optic nerves.

The eddy current distortion was corrected using FuncTool software when calculating the FA maps. Post-processing involving coregistering the diffusion weighted images to a reference image (Wei et al., 2012, *Comput Med Imaging Graph.)*. No special algorithm was used to register the T2WI to the FA maps, but we used a fusion function in DICOM image viewer (OsiriX MD). Using this method, there were no problematic misalignments between the T2WI and FA maps. The ROIs were manually drawn on the T2WI and, using the same coordinates, applied to the FA maps. The FA values obtained within the ROI (drawn on the FA map) are averages.

Representative images the optic nerves of a normal and glaucomatous eye are shown in Figure 1C. A decreased FA value from control values in this study suggests decreased diffusion directivity of the optic nerve [28].

2.5. Exclusions

One week following the second laser photocoagulation, the IOP of three macaques did not increase beyond normal IOP. Thus, these three macaques were not utilized in the current study and returned to the in-house colony.

2.6. Statistical analysis

The current study was carried out in a completely randomized design with a single factor. Macaques were randomly assigned after the second laser treatment to either brimonidine or control treatment groups such that there were no differences in average IOP between the two groups. Ocular parameters were measured in a non-blinded manner. Ocular parameters before laser treatment were normal. Data were expressed as mean ± S.E.M. Comparisons within and between treatment groups over time was performed using repeated measures two-way analysis of variance (ANOVA). Data were analyzed using statistical analysis software SAS System Version 9.4 (SAS Institute Inc., Cary, NC). *P* values at less than 0.05 were considered statistically significant.

3. Results

3.1. Intraocular pressure over time and the effect of brimonidine on IOP

The mean (±S.E.M.) IOP before laser photocoagulation was 18.0 ± 0.4 mmHg (Figure 2A, B). Beginning one week following the second photocoagulation, IOP significantly increased in the ipsilateral eye (54.1 ± 4.0 mmHg) compared to pre-photocoagulation ($p < 0.05$ vs. Week 0). In addition, at one week following the second photocoagulation, IOP was significantly increased compared to the contralateral, normotensive eye (17.0 ± 0.7 mmHg) ($p < 0.05$). Intraocular pressure of the contralateral eyes did not significantly change over time.

Intraocular pressure of the glaucomatous eyes, treated with either artificial tears or brimonidine, measured before the first daily dose, remained elevated for the duration of the study. A two-way repeated measures ANOVA was conducted to compare the effects of artificial tears and brimonidine treatment on IOP of the glaucomatous eyes over time. No significant effects on IOP with either treatment over time were observed ($F(5, 48) = 0.735$, $p = 0.601$).

3.2. Vertical C/D ratio over time and the effect of brimonidine on vertical C/D

The mean vertical C/D ratio before laser photocoagulation was 0.46 ± 0.01 (Figure 2C, D). Beginning one week following the second laser treatment, vertical C/D ratio significantly increased in the ipsilateral eye (0.7 ± 0.03) compared to pre-photocoagulation ($p < 0.05$ vs. Week 0). Vertical C/D ratio of the ipsilateral eye at one week following the second photocoagulation was also significantly increased compared to the contralateral, control eye (0.48 ± 0.02) ($p < 0.05$). Vertical C/D of the contralateral eye did not significantly change over time.

Vertical C/D ratio of glaucomatous eyes, treated with either artificial tears or brimonidine, remained elevated for the duration of the study. A two-way repeated measures ANOVA was conducted to compare the effects of artificial tears and brimonidine treatment on vertical C/D ratio of glaucomatous eyes over time. No significant effects on vertical C/D with either treatment over time were observed ($F(5, 42) = 1.877$, $p = 0.119$).

3.3. Minimum R/D ratio over time and the effect of brimonidine on minimum R/D ratio

The mean minimum R/D ratio before laser photocoagulation was 0.19 ± 0.01 (Figure 2E, F). Beginning one week following the second laser treatment, minimum R/D ratio significantly decreased in the ipsilateral eye (0.08 ± 0.01) compared to pre-photocoagulation ($p < 0.05$ vs.

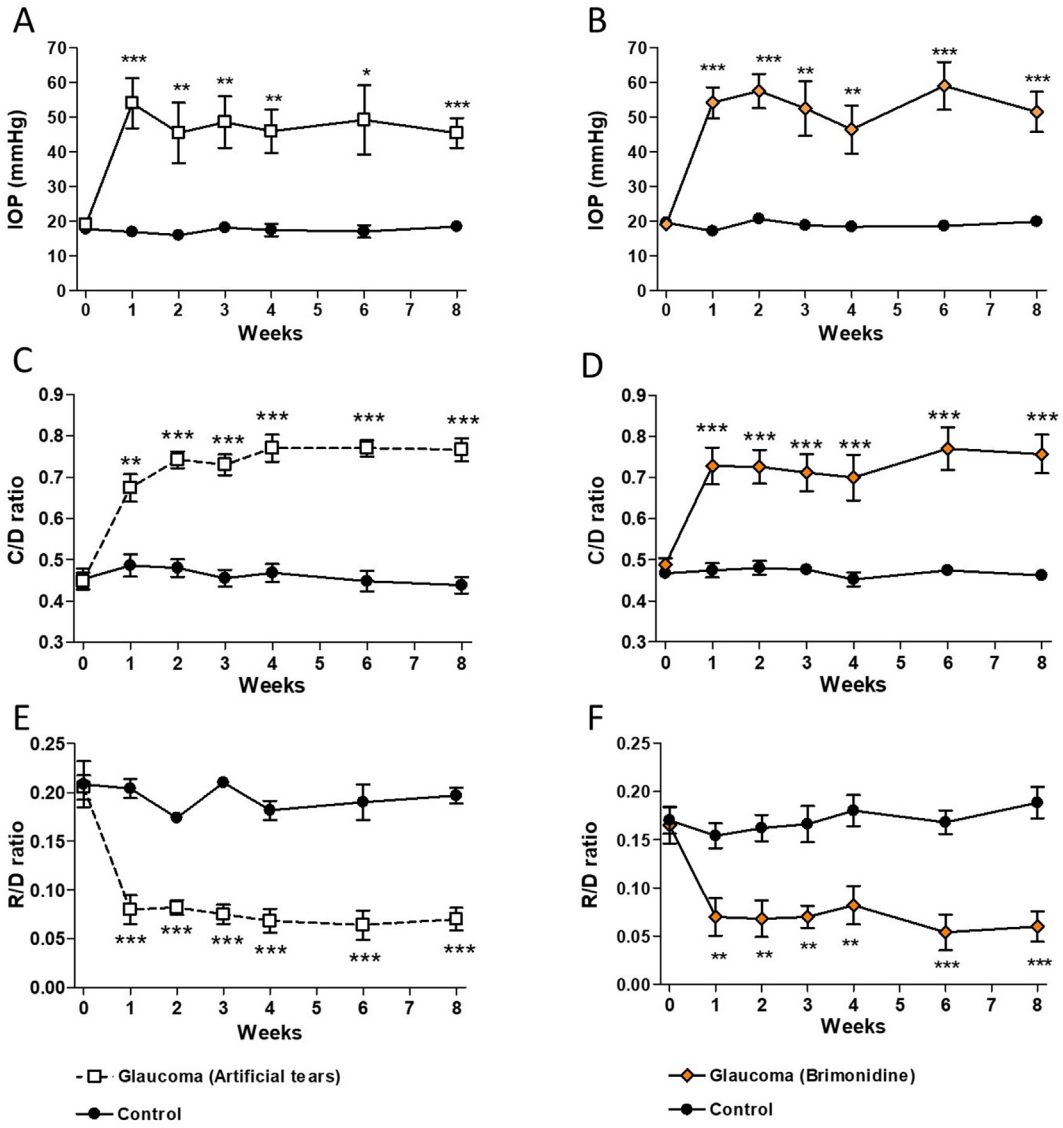

Figure 2. Intraocular pressure (IOP), vertical cup-to-disc (C/D) ratio and minimum rim-to-disc (R/D) ratio over time following laser photocoagulation of the trabecular meshwork of one eye in macaques. The contralateral eye served as a normotensive control. (A, B) IOP (C, D) vertical C/D ratio and (E, F) minimum R/D ratio were measured prior to laser treatment and then 1, 2, 3, 4, 6 and 8 weeks following the second laser treatment. Data are presented as mean ± S.E.M. N = 6 per treatment group. $^{*}P < 0.05$, $^{**}P < 0.01$, $^{***}P < 0.001$ compared to the control eye.

Week 0). Minimum R/D ratio of the ipsilateral eye at one week following the second photocoagulation was also significantly decreased compared to the contralateral, control eye (0.18 ± 0.01) ($p < 0.05$). Minimum R/D ratio of contralateral eyes did not significantly change over time.

Minimum R/D ratio of glaucomatous eyes, treated with either artificial tears or brimonidine, remained decreased for the duration of the study. A two-way repeated measures ANOVA was conducted to compare the effects of artificial tears and brimonidine treatment on minimum R/D ratio of glaucomatous eyes over time. No significant effects on minimum R/D ratio with either treatment were over time were observed ($F(5, 42) = 0.360$, $p = 0.873$).

3.4. RNFL thickness over time and the effect of brimonidine on RNFL thickness

Before photocoagulation, mean RNFL thickness of all animals was 104.3 ± 1.7 μm (Figure 3A, 3B). One and two weeks following the second laser treatment, in both brimonidine and artificial tears treated eyes, RNFL thickness decreased slightly compared to the contralateral, control eye. Beginning three weeks after the second photocoagulation, significantly decreased RNFL thickness was observed, which persisted for at least eight weeks ($p < 0.05$ vs. contralateral eye). Retinal nerve fiber layer thickness of the contralateral, control eye did not change over time (Figure 3A, 3B).

No significant interaction between treatment groups and time was observed ($F(42, 63) = 0.724$, $p = 0.609$). However, a significant effect of time was observed ($F(5, 63) = 18.734$, $p < 0.001$). While mean RNFL thickness values of both treatment groups decreased over time, RNFL thickness of brimonidine treated eyes tended to be greater than those of the artificial tears treated eyes throughout the study period (Figure 3C). Significantly decreased RNFL in artificial tears-treated eyes was observed beginning three weeks after the second photocoagulation ($p < 0.05$). By contrast, significant decreases in RNFL thickness in brimonidine treated eyes were observed much later, at six and eight weeks after the second laser treatment ($p < 0.05$). At four weeks, mean RNFL thickness tended to be greater in the brimonidine-treated eyes compared to artificial tears-treated eyes ($p = 0.065$). By eight weeks, the mean RNFL thickness of the eyes treated with artificial tears was 56.8 ± 7.0 μm, whereas the

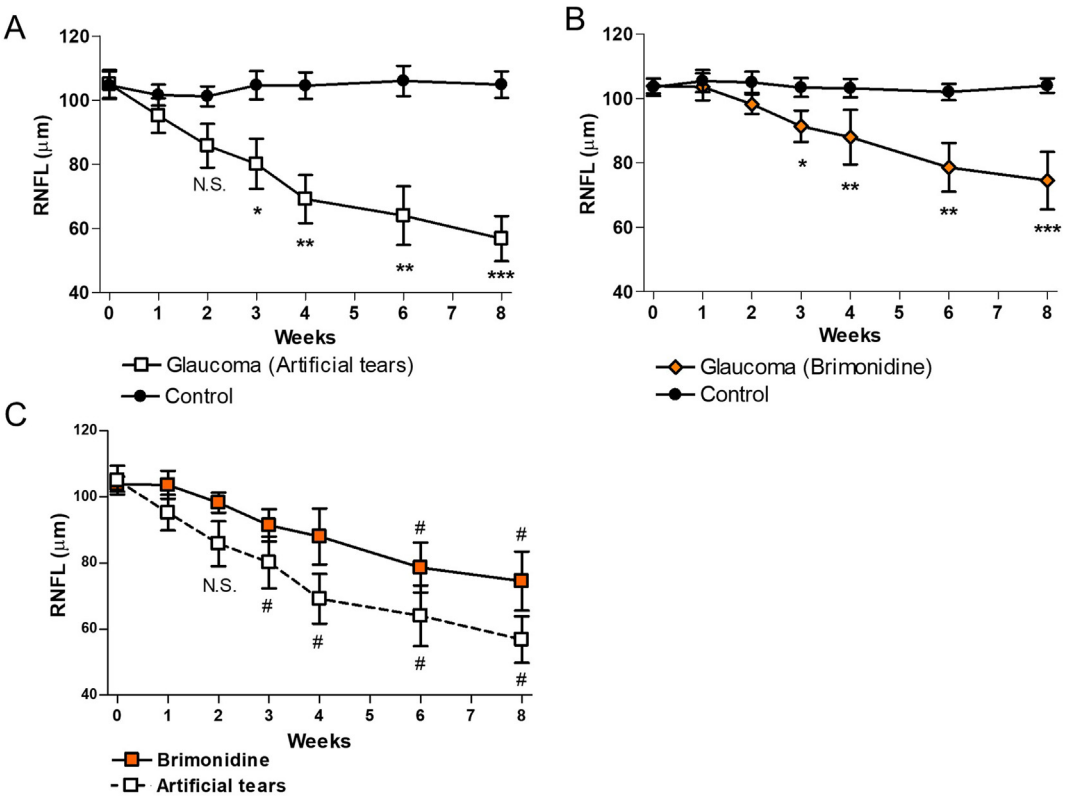

Figure 3. Retinal nerve fiber layer (RNFL) thickness over time following photocoagulation of the trabecular meshwork of one eye in macaques. The contralateral eye served as a normotensive control. Either (A) artificial tears or (B) brimonidine was instilled, twice daily in both the glaucomatous and control eyes. Measurements of RNFL thickness were performed prior to photocoagulation, and then 1, 2, 3, 4, 6 and 8 weeks following the second laser photocoagulation. $^{*}P < 0.05$, $^{**}P < 0.01$, $^{***}P < 0.001$ compared to the normotensive eye. N.S.: Not significant. (C) Effect over time of either brimonidine or artificial tears treatment on RNFL thickness in glaucomatous eyes. $\#P < 0.05$ compared to Week 1 within each treatment group. Data are presented as mean ± S.E.M. N = 5–6 per treatment group.

mean RNFL thickness of brimonidine-treatment eyes was 74.5 ± 8.9 μm. At eight weeks, the man RNFL thicknesses of brimonidine-treated eyes tended to be thicker than that of eyes treated with artificial tears ($p = 0.079$).

3.5. FA over time and the effect of brimonidine on FA

Before photocoagulation, mean FA from all animals was 0.34 ± 0.01 (Figure 4A, B). One week following the second photocoagulation, FA of the brimonidine-treated and artificial tears-treated eyes was not significantly different compared to the contralateral, control eye ($p > 0.05$). Beginning two weeks after the second laser treatment, FA of eyes treated with artificial tears significantly decreased compared to the control eye and this reduction persisted for at least eight weeks ($p < 0.05$ vs. contralateral eye; Figure 4A). By contrast, while tending to be lower compared to the control eye, FA of glaucomatous eyes treated with brimonidine was not significantly different from that of control eyes (Figure 4B). The FA of the contralateral eyes, from either artificial tears or brimonidine groups, did not change over time.

A statistically significant interaction between treatment groups and time was observed ($F(5, 69) = 2.794$, $p = 0.027$). As described earlier, while FA of brimonidine-treated eyes tended to decrease over time, at no time was FA significantly decreased compared to FA at the start of treatment ($p > 0.05$ vs. Week 1; Figure 4C). By contrast, a gradual decrease of FA was observed in artificial tears-treated eyes over time ($p < 0.05$ vs. Week 1; Figure 4C).

3.6. Short-term IOP time course after brimonidine instillation

To confirm that acute brimonidine treatment acutely lowers IOP in glaucomatous macaques, the effect of brimonidine on IOP was examined over a 10-h period (Figure 5). Overall, a statistically significant interaction between brimonidine treatment over time was observed ($F(7, 42) = 4.459$, $p = 0.0009$). The first treatment of brimonidine tended to reduce IOP, between 10 and 20 mmHg, one and 2 h following treatment, respectively. Significant lowering of IOP was observed 4 h after treatment ($p < 0.05$ vs. artificial tears treatment). A second dose of brimonidine was administered 8 h after the first dose. Following the second dose of brimonidine, significantly decreased IOP was observed 1 and 2 h after dosing (or 9 and 10 h after the first dose of brimonidine) ($p < 0.05$ vs. artificial tears treatment). Intraocular pressure of glaucomatous eyes treated with artificial tears did not significantly change over time ($p > 0.05$ vs. pre-instillation, 0 h; Figure 5).

4. Discussion

The current study provides evidence that SD-OCT and DTI could be useful for quantitative longitudinal evaluation of optic nerve neuropathy. While both imaging modalities detected the presence of RGC axonal degeneration, axonal degeneration appeared to be observed sooner with DTI comparted to SD-OCT. Both imaging modalities also revealed delayed axonal degeneration with brimonidine treatment. Over time, however, RNFL thickness markedly decreased below pre-hypertensive thickness. By contrast, optic nerve FA in brimonidine-treated macaques did not significantly decrease over time. The current findings show that both imaging modalities could be utilized to longitudinally track neuroprotection. A combination of these imaging modalities could be useful in detecting early neuropathy, tracking disease progression and demonstrating neuroprotection of novel treatments over time.

While widely utilized as a means of detecting and tracking glaucomatous neuropathy, optic nerve head topography has limitations as there is considerable variation in optic nerve head cupping among

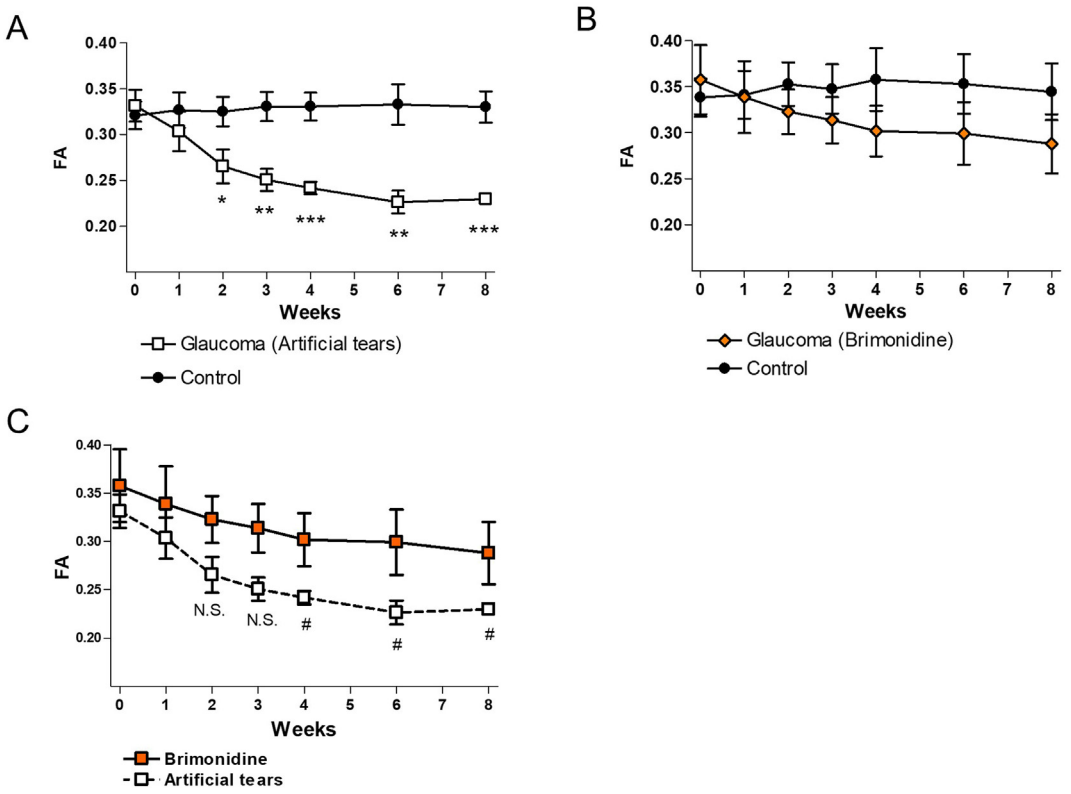

Figure 4. Fractional anisotropy (FA) over time following photocoagulation of the trabecular meshwork of one eye in macaques and representative axial MR images of the macaque eyes. The untreated eye served as a normotensive control. Either (A) artificial tears or (B) brimonidine was instilled, twice daily in both the glaucomatous and the contralateral normotensive eyes. Fractional anisotropy was measured prior to photocoagulation, and then 1, 2, 3, 4, 6 and 8 weeks following the second laser photocoagulation. $*P < 0.05$, $**P < 0.01$, $***P < 0.001$ compared to artificial tears treatment. N.S.: Not significant. (C) Effect over time of either brimonidine or artificial tears treatment on FA in glaucomatous eyes. $\#P < 0.05$ compared to Week 1 within each treatment group. Data are presented as mean ± S.E.M. N = 5–6 per treatment group.

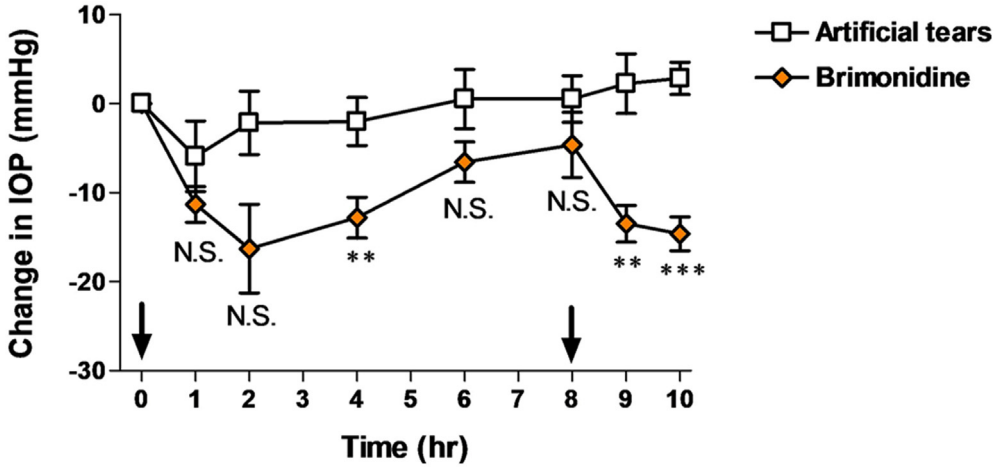

Figure 5. Change in intraocular pressure (IOP) following treatment with either brimonidine or artificial tears over time of the glaucomatous eye. Change in IOP was calculated by subtracting IOP after treatment from that before treatment (at 0 h). Arrows indicate a single instillation of either brimonidine or artificial tears. Data are presented as mean ± S.E.M. N = 4 per treatment group. $**P < 0.01$, $***P < 0.001$ compared to artificial tears treatment. N.S.: Not significant.

glaucoma patients. In addition, changes in topography, such as C/D and R/D ratio may not be adequately sensitive to detect low grade RGC axonal degeneration—marked degeneration may have already occurred and neuroprotective treatment may not have any efficacy on advanced neuropathy [9,29,30,31]. On one hand, OCT could be utilized as a noninvasive and quantitative method of assessing RGC degeneration [32, 33]. However, the sensitivity of OCT to predict future visual field loss in preperimetric glaucoma patients is low [13].

On the other hand, DTI could be used specifically to detect early structural deficits before significant visual field loss. Decreased intra-orbital optic nerve diameter and cross sectional area, obtained with T2-weighed MRI, have demonstrated the ability to distinguish between mild and advanced glaucoma [34]. Differentiating between patients with mild glaucoma and normal controls has also been demonstrated and function, as determined by visual field testing, correlated with T2-weighted optic nerve images, unlike that with optic nerve head

topography [34]. Diffusion tensor imaging provides greater information concerning tissue pathology than T2 imaging alone. In control-treated ocular hypertensive eyes in the current study, decreased FA was observed before significant RNFL thinning, indicating that optic nerve axon degeneration began prior to the loss of axons that comprise the RNFL [35,36]. Cell bodies and proximal axons appear to survive through uninjured collateral axonal branches [35]. Permanent structural deformation to the lamina cribrosa has been suggested as having a key role in mediating axonal injury including glaucoma cases without elevated IOP [36]. Similar to findings in the current study, optic nerves of glaucoma patients show lower than normal FA. Significant associations between FA and glaucoma severity have been reported, suggesting utility of FA as a morphometric marker of visual functioning [14,15,37]. While not tested in the current study, it is likely that the control-treated ocular hypertensive macaques have diminished visual field functioning, as these macaques demonstrated both significantly decreased RNFL thickness and decreased FA [38]. Thus, visualizing intraorbital optic nerve pathology could be useful in detecting early stage glaucoma.

One other limitation of optic nerve head topography as an outcome measure is its potential lack of sensitivity to therapeutic intervention. While there are a number of preclinical studies that have shown reduced or delayed loss of RGC with putative neuroprotective treatments, few, if any, clinical glaucoma studies have demonstrated significant improvement in optic nerve head topography during a neuroprotective treatment [39,40,41]. The lack of change in optic nerve head topography does not address whether a treatment was in fact neuroprotective or not.

Likewise, no effect on C/D and R/D ratios with brimonidine treatment was observed in the current study. However, brimonidine treatment appeared to delay decreases in FA and RNFL thickness compared to vehicle-treated eyes. The current preclinical findings mirror those of a clinical study that evaluated the effect of brimonidine on RNFL thickness in glaucoma patients [42]. Tsai and Chang performed funduscopy and measured RNFL thickness with scanning laser polarimetry over a 12-month period; no funduscopy results were reported. The authors reported significant decreases of IOP following 12 months of treatment with either brimonidine and a comparator, timolol, a β-adrenergic antagonist. Eyes treated with timolol showed decreases in RNFL thickness overall and within each of the four quadrants. However, there was no significant change in RNFL thickness after brimonidine treatment, indicating a potential neuroprotective effect independent of IOP reduction.

While Tsai and Chang reported no significant change in RNFL thickness in brimonidine-treated eyes, the current study observed a gradual decline in RNFL thickness—at six weeks, RNFL thickness of the brimonidine-treated eye was less than that compared to pre-laser trabeculoplasty baseline. By contrast, RNFL thickness of control-treated eyes were less than baseline beginning at three weeks. The loss in RNFL thickness in patients treated with timolol [42] was about 4% over 12 months whereas a loss of about 40% was observed in the current study at eight weeks. One difference between the current study and that of Tsai and Chang is that scanning laser polarimetry was used. However, there is a close correspondence of RNFL thickness measured with scanning laser polarimetry and OCT [43]. Alternatively, the rapid decrease in RNFL thickness observed in the macaques could be due to the acute and rapid increase of IOP. The extent to which rapid neurodegeneration in macaques mirrors the gradual pathophysiology observed in clinical glaucomatous neurodegeneration needs further elucidation.

With respect to brimonidine's potential neuroprotective effect, perhaps a higher concentration of brimonidine (0.2%) [42], compared to the current study (0.1%) could have further delayed RNFL thinning in the macaques. Nonetheless, the current findings tend to support the clinical findings, in that brimonidine has a neuroprotective effect likely separate from reduced IOP. The current findings, of a delay in optic nerve degeneration compared to that of control-treated eyes, further support a neuroprotective role of brimonidine. The current findings further suggest a role of DTI as a preclinical morphometric tool for assessing neuroprotective effects of potential treatments.

While DTI could be utilized as a noninvasive method of morphometric optic nerve analysis, a number of technical aspects will need clarification, such as reducing signal contamination from fat and CSF found within the optic nerve. There is currently no standard DTI protocol for the optic nerve and this lack of standardization is apparent in differences between studies in signal-to-noise ratio and in normative FA values [14]. Distinguishing aging-related changes in optic nerve that are not due to glaucoma has yet to be fully addressed—the current study utilized young macaques. Also, while current FA measurements mathematically suggest decreased structural integrity of "nerve tissue", it is currently not feasible to assign changes specifically in axons and changes specifically in myelin. Thus, more in-depth studies of DTI as a means of quantitative morphometry are needed. There are other drawbacks in general with MRI. Physiological noise, including "vessel pulsation, respiration and head movement" reduces image resolution [34]. To minimize movement, macaques were anesthetized and the head was fixed in a head holder. Nonetheless, the resolution of one voxel is 1 mm, whereas it is possible to discern the different cell layers of the retina with OCT—the average thickness of the RNFL in young adults is about 93 μm [44]. Rather than one modality over another, DTI and SD-OCT could be utilized to provide complementary structural data.

Greater utilization of morphometric analysis of RGC degeneration for early disease detection and progression over time, as well as for treatment efficacy monitoring, is needed. However, morphometry of the macula, for example, will need further methodological refinement before widespread use as a clinical assessment method. Age-related loss of retinal ganglion cells varies between individuals as well as within a given macula [45]. The region of interest for macular OCT has yet to be fully established and there does not appear to be outcome measures other than macular thickness to reflect changes in tissue mophometry [45]. These challenges, though, could be refined in a non-human animal model, as subject age, disease onset and severity are defined at the outset. In the few studies that have examined macular thickness in NHP, both no change and significant changes were reported [46,47].

Declarations

Author contribution statement

Nobuyuki Takahashi: Conceived and designed the experiments; Performed the experiments; Analyzed and interpreted the data; Wrote the paper.

Naoko Matsunaga, Aldric Hama: Analyzed and interpreted the data; Wrote the paper.

Takahiro Natsume: Conceived and designed the experiments; Performed the experiments; Analyzed and interpreted the data.

Chinatsu Kitazawa, Yoshitaka Itani: Conceived and designed the experiments; Performed the experiments.

Ikuo Hayashi, Masamitsu Shimazawa, Hideaki Hara: Analyzed and interpreted the data.

Hiroyuki Takamatsu: Conceived and designed the experiments; Analyzed and interpreted the data.

Funding statement

This research did not receive any specific grant from funding agencies in the public, commercial, or not-for-profit sectors.

Data availability statement

Data will be made available on request.

Declaration of interests statement

Nobuyuki Takahashi, Naoko Matsunaga, Chinatsu Kitazawa, Yoshitaka Itani, Aldric Hama, Ikuo Hayashi, Hiroyuki Takamatsu and Masamitsu Shimazawa are employees of Hamamatsu Pharma Research.

Additional information

No additional information is available for this paper.

Acknowledgements

The authors gratefully acknowledge the HPR animal care team for expert animal care. We also thank Dr. Rintaro Fujii for technical assistance and advice.

References

[1] H.A. Quigley, A.T. Broman, The number of people with glaucoma worldwide in 2010 and 2020, Br. J. Ophthalmol. 90 (3) (2006) 262–267.
[2] A.C. Kara-Jose, L.A.S. Melo Jr., B.L.B. Esporcatte, A. Endo, M.T. Leite, I.M. Tavares, The disc damage likelihood scale: diagnostic accuracy and correlations with cup-to-disc ratio, structural tests and standard automated perimetry, PloS One 12 (7) (2017), e0181428.
[3] M. Lawlor, H. Danesh-Meyer, L.A. Levin, I. Davagnanam, E. De Vita, G.T. Plant, Glaucoma and the brain: trans-synaptic degeneration, structural change, and implications for neuroprotection, Surv. Ophthalmol. 63 (3) (2018) 296–306.
[4] A. Doozandeh, S. Yazdani, Neuroprotection in glaucoma, J. Ophthalmic Vis. Res. 11 (2) (2016) 209–220.
[5] R. Nuzzi, L. Dallorto, T. Rolle, Changes of visual pathway and brain connectivity in glaucoma: a systematic review, Front. Neurosci. 12 (2018) 363.
[6] C.C. Boucard, S. Hanekamp, B. Curcic-Blake, M. Ida, M. Yoshida, F.W. Cornelissen, Neurodegeneration beyond the primary visual pathways in a population with a high incidence of normal-pressure glaucoma, Ophthalmic Physiol. Opt. 36 (3) (2016) 344–353.
[7] D.F. Sena, K. Lindsley, Neuroprotection for treatment of glaucoma in adults, Cochrane Database Syst. Rev. 1 (2017) CD006539.
[8] C. Ergorul, L.A. Levin, Solving the lost in translation problem: improving the effectiveness of translational research, Curr. Opin. Pharmacol. 13 (1) (2013) 108–114.
[9] H.D. Jampel, D. Friedman, H. Quigley, S. Vitale, R. Miller, F. Knezevich, et al., Agreement among glaucoma specialists in assessing progressive disc changes from photographs in open-angle glaucoma patients, Am. J. Ophthalmol. 147 (1) (2009) 39–44 e31.
[10] A.J. Tatham, R.N. Weinreb, L.M. Zangwill, J.M. Liebmann, C.A. Girkin, F.A. Medeiros, The relationship between cup-to-disc ratio and estimated number of retinal ganglion cells, Invest. Ophthalmol. Vis. Sci. 54 (5) (2013) 3205–3214.
[11] J.C. Mwanza, J.L. Warren, D.L. Budenz, Utility of combining spectral domain optical coherence tomography structural parameters for the diagnosis of early Glaucoma: a mini-review, Eye Vis (Lond) 5 (2018) 9.
[12] A.J. Tatham, F.A. Medeiros, Detecting structural progression in glaucoma with optical coherence tomography, Ophthalmology 124 (12S) (2017) S57–S65.
[13] A.H. Marvasti, A.J. Tatham, L.M. Zangwill, C.A. Girkin, J.M. Liebmann, R.N. Weinreb, et al., The relationship between visual field index and estimated number of retinal ganglion cells in glaucoma, PloS One 8 (10) (2013), e76590.
[14] S.T. Chang, J. Xu, K. Trinkaus, M. Pekmezci, S.N. Arthur, S.K. Song, et al., Optic nerve diffusion tensor imaging parameters and their correlation with optic disc topography and disease severity in adult glaucoma patients and controls, J. Glaucoma 23 (8) (2014) 513–520.
[15] S. Sidek, N. Ramli, K. Rahmat, N.M. Ramli, F. Abdulrahman, L.K. Tan, Glaucoma severity affects diffusion tensor imaging (DTI) parameters of the optic nerve and optic radiation, Eur. J. Radiol. 83 (8) (2014) 1437–1441.
[16] K. Li, C. Lu, Y. Huang, L. Yuan, D. Zeng, K. Wu, Alteration of fractional anisotropy and mean diffusivity in glaucoma: novel results of a meta-analysis of diffusion tensor imaging studies, PloS One 9 (5) (2014), e97445.
[17] T. Hayashi, M. Shimazawa, H. Watabe, T. Ose, Y. Inokuchi, Y. Ito, et al., Kinetics of neurodegeneration based on a risk-related biomarker in animal model of glaucoma, Mol. Neurodegener. 8 (2013) 4.
[18] G. Pihl-Jensen, M.F. Schmidt, J.L. Frederiksen, Multifocal visual evoked potentials in optic neuritis and multiple sclerosis: a review, Clin. Neurophysiol. 128 (7) (2017) 1234–1245.
[19] L.B. Cantor, Brimonidine in the treatment of glaucoma and ocular hypertension, Therapeut. Clin. Risk Manag. 2 (4) (2006) 337–346.
[20] L.A. Wheeler, R. Lai, E. Woldemussie, From the lab to the clinic: activation of an alpha-2 agonist pathway is neuroprotective in models of retinal and optic nerve injury, Eur. J. Ophthalmol. 9 (Suppl 1) (1999) S17–21.
[21] D. Lee, K.Y. Kim, Y.H. Noh, S. Chai, J.D. Lindsey, M.H. Ellisman, et al., Brimonidine blocks glutamate excitotoxicity-induced oxidative stress and preserves mitochondrial transcription factor a in ischemic retinal injury, PloS One 7 (10) (2012), e47098.
[22] L. Wheeler, E. WoldeMussie, R. Lai, Role of alpha-2 agonists in neuroprotection, Surv. Ophthalmol. 48 (Suppl 1) (2003) S47–51.
[23] K.I. Jung, J.H. Kim, C.K. Park, alpha2-Adrenergic modulation of the glutamate receptor and transporter function in a chronic ocular hypertension model, Eur. J. Pharmacol. 765 (2015) 274–283.
[24] W.S. Lambert, L. Ruiz, S.D. Crish, L.A. Wheeler, D.J. Calkins, Brimonidine prevents axonal and somatic degeneration of retinal ganglion cell neurons, Mol. Neurodegener. 6 (1) (2011) 4.
[25] Institute for Laboratory Animal Research, Guide for the Care and Use of Laboratory Animals, eighth ed., The National Academies Press, Washington, D.C., 2011.
[26] M. Shimazawa, G. Tomita, T. Taniguchi, M. Sasaoka, H. Hara, Y. Kitazawa, et al., Morphometric evaluation of changes with time in optic disc structure and thickness of retinal nerve fibre layer in chronic ocular hypertensive monkeys, Exp. Eye Res. 82 (3) (2006) 427–440.
[27] H.A. Quigley, R.M. Hohman, Laser energy levels for trabecular meshwork damage in the primate eye, Invest. Ophthalmol. Vis. Sci. 24 (9) (1983) 1305–1307.
[28] P.J. Basser, J. Mattiello, D. LeBihan, MR diffusion tensor spectroscopy and imaging, Biophys. J. 66 (1) (1994) 259–267.
[29] M.T. Nicolela, S.M. Drance, Various glaucomatous optic nerve appearances: clinical correlations, Ophthalmology 103 (4) (1996) 640–649.
[30] M.T. Nicolela, T.A. McCormick, S.M. Drance, S.N. Ferrier, R.P. LeBlanc, B.C. Chauhan, Visual field and optic disc progression in patients with different types of optic disc damage: a longitudinal prospective study, Ophthalmology 110 (11) (2003) 2178–2184.
[31] S. Narayan, R. Sreekumari, Comparison of vertical cup-disc ratio and disc damage likelihood scale with respect to visual field global indices in primary open-angle glaucoma patients: a cross-sectional study, Kerala J Ophthalmol 29 (2) (2017) 91–96.
[32] J.C. Mwanza, G. Lee, D.L. Budenz, J.L. Warren, M. Wall, P.H. Artes, et al., Validation of the UNC OCT index for the diagnosis of early glaucoma, Translat. Vis. Sci. Techn. 7 (2) (2018) 16.
[33] R.S. Harwerth, J.L. Wheat, M.J. Fredette, D.R. Anderson, Linking structure and function in glaucoma, Prog. Retin. Eye Res. 29 (4) (2010) 249–271.
[34] R.L. Furlanetto, S.H. Teixeira, C.P.B. Gracitelli, C.L. Lottenberg, F. Emori, M. Michelan, et al., Structural and functional analyses of the optic nerve and lateral geniculate nucleus in glaucoma, PloS One 13 (3) (2018), e0194038.
[35] R. Adalbert, M.P. Coleman, Review: axon pathology in age-related neurodegenerative disorders, Neuropathol. Appl. Neurobiol. 39 (2) (2013) 90–108.
[36] K. Evangelho, M. Mogilevskaya, M. Losada-Barragan, J.K. Vargas-Sanchez, Pathophysiology of primary open-angle glaucoma from a neuroinflammatory and neurotoxicity perspective: a review of the literature, Int. Ophthalmol. 39 (1) (2019) 259–271.
[37] M.Y. Wang, K. Wu, J.M. Xu, J. Dai, W. Qin, J. Liu, et al., Quantitative 3-T diffusion tensor imaging in detecting optic nerve degeneration in patients with glaucoma: association with retinal nerve fiber layer thickness and clinical severity, Neuroradiology 55 (4) (2013) 493–498.
[38] W.A. Hare, E. WoldeMussie, R.K. Lai, H. Ton, G. Ruiz, T. Chun, et al., Efficacy and safety of memantine treatment for reduction of changes associated with experimental glaucoma in monkey, I: functional measures, Invest. Ophthalmol. Vis. Sci. 45 (8) (2004) 2625–2639.
[39] N.N. Osborne, G. Chidlow, C.J. Layton, J.P. Wood, R.J. Casson, J. Melena, Optic nerve and neuroprotection strategies, Eye 18 (11) (2004) 1075–1084.
[40] W.A. Hare, E. WoldeMussie, R.N. Weinreb, H. Ton, G. Ruiz, M. Wijono, et al., Efficacy and safety of memantine treatment for reduction of changes associated with experimental glaucoma in monkey, II: structural measures, Invest. Ophthalmol. Vis. Sci. 45 (8) (2004) 2640–2651.
[41] R.N. Weinreb, J.M. Liebmann, G.A. Cioffi, I. Goldberg, J.D. Brandt, C.A. Johnson, et al., Oral memantine for the treatment of glaucoma: design and results of 2 randomized, placebo-controlled, phase 3 studies, Ophthalmology 125 (12) (2018) 1874–1885.
[42] J.C. Tsai, H.W. Chang, Comparison of the effects of brimonidine 0.2% and timolol 0.5% on retinal nerve fiber layer thickness in ocular hypertensive patients: a prospective, unmasked study, J. Ocul. Pharmacol. Therapeut. 21 (6) (2005) 475–482.
[43] T. Diekmann, L.M. Schrems-Hoesl, C.Y. Mardin, R. Laemmer, F.K. Horn, F.E. Kruse, et al., Predictive factors for visual field conversion: comparison of scanning laser polarimetry and optical coherence tomography, J. Glaucoma 27 (2) (2018) 157–163.
[44] J.W. Jang, M.W. Lee, K.J. Cho, Comparative analysis of mean retinal thickness measured using SD-OCT in normal young or old age and glaucomatous eyes, Int. Ophthalmol. 38 (6) (2018) 2417–2426.
[45] K. Nouri-Mahdavi, R.E. Weiss, Detection of glaucoma deterioration in the macular region with optical coherence tomography: challenges and solutions, Am. J. Ophthalmol. 222 (2020) 277–284.
[46] S. Liu, B. Wang, B. Yin, T.E. Milner, M.K. Markey, S.J. McKinnon, et al., Retinal nerve fiber layer reflectance for early glaucoma diagnosis, J. Glaucoma 23 (1) (2014) e45–52.
[47] L.J. Wilsey, J. Reynaud, G. Cull, C.F. Burgoyne, B. Fortune, Macular structure and function in nonhuman primate experimental glaucoma, Invest. Ophthalmol. Vis. Sci. 57 (4) (2016) 1892–1900.